Наносистеми, наноматеріали, нанотехнології
Nanosistemi, Nanomateriali, Nanotehnologii
2025, т. 23, № 3, сс. 733–747
https://doi.org/10.15407/nnn.23.03.0733

© 2025 ІМФ (Інститут металофізики
ім. Г. В. Курдюмова НАН України)
Надруковано в Україні.

PACS numbers: 61.05.cf, 61.46.Hk, 62.25.Mn, 64.75.Jk, 68.37.Hk, 78.67.Bt, 81.05.Pj

Features of Formation of Optically Transparent Nanostructured Spinel-Containing Glass-Ceramic Materials

O. V. Savvova, O. H. Tur, M. M. Hozha, O. V. Babich, O. I. Fesenko, V. V. Bielov, and Yu. O. Smyrnova

O. M. Beketov National University of Urban Economy in Kharkiv,
17, Marshal Bazhanov Str.,
UA-61002 Kharkiv, Ukraine

The main conditions for the formation of the sitallized nanostructure of glass-ceramic materials based on spinel containing Co^{2+} ions with high absorption in the range of 1.6–1.7 μm for laser shutters operating in the mode of passive *Q*-switched are determined: the presence of phase-forming oxides $\Sigma(MgO, Al_2O_3) = 40.0$ wt.%, glass-forming oxides $\Sigma(B_2O_3, SiO_2) = 54.0$ wt.%, crystallization catalysts $\Sigma(P_2O_5, ZnO, ZrO_2, TiO_2, CeO_2, Sb_2O_3) = 4.9$ wt.%, modifying additives $\Sigma(SrO, BaO, CaO, CoO) = 1.1$ wt.%.; glass melting at a temperature of 1550°C for 6 hours; three-stage heat treatment (I stage—800°C, $\tau = 1$ h; II stage—900°C, $\tau = 30$ min; III stage—950°C, $\tau = 5$ min). As established, ensuring high values of light transmission ($T = 74\%$) and crack resistance ($K_{1C} = 5.0$ MPa·m$^{1/2}$) of glass-ceramic material is realized due to the following stages: metastable phase immiscibility by the mechanism of spinodal decomposition (800°C), intensification of nucleation (850°C) while keeping the bidispersity of the system and providing the structural stability of the glass with kinetic inhibition of the crystal growth process under conditions of high viscosity, formation of solid solutions with the structure of high-temperature quartz in the low-temperature region (900°C) and spinel crystals of 50 nm in size in the amount of 50 vol.% (950°C) with a regular distribution of nanocrystals in the residual glass phase.

Визначено основні умови формування ситалізованої наноструктури склокристалічних матеріялів на основі шпінелі, що містять йони Co^{2+}, з високим вбиранням у діяпазоні 1,6–1,7 мкм для лазерних заслінок, які функціонують у режимі пасивної модуляції добротности: наявність фазоутворювальних оксидів $\Sigma(MgO, Al_2O_3) = 40{,}0$ мас.%, склоутворювальних оксидів $\Sigma(B_2O_3, SiO_2) = 54{,}0$ мас.%, каталізаторів кристалізації $\Sigma(P_2O_5, ZnO, ZrO_2, TiO_2, CeO_2, Sb_2O_3) = 4{,}9$ мас.%, модифікувальних добавок $\Sigma(SrO, BaO, CaO, CoO) = 1{,}1$ мас.%; вариво стекол за температури у 1550°C упродовж 6 год; тристадійне термооброблення (I стадія за

800°C, $\tau = 1$ год; II стадія за 900°C, $\tau = 30$ хв; III стадія за 950°C, $\tau = 5$ хв). Встановлено, що забезпечення високих значень світлопроникности ($T = 74\%$) і показника тріщиностійкости ($K_{1C} = 5{,}0$ МПа·м$^{1/2}$) склокристалічного матеріялу реалізується за рахунок стадій: метастабільного фазового незмішування за механізмом спинодального розпаду (800°C), інтенсифікації зародкоутворення (850°C) із збереженням бідисперсности системи та забезпеченням структурної стійкости скла з кінетичним гальмуванням процесу росту в умовах підвищеної в'язкости, формування твердих розчинів зі структурою високотемпературного кварцу в низькотемпературній області (900°C) та кристалів шпінелі розміром у 50 нм у кількості 50 об.% (950°C) з реґулярним характером розподілу нанокристалів у залишковій склофазі.

Key words: glass-ceramic materials, magnesium-aluminosilicate glasses, spinel, nanostructure, light transmission, crack resistance.

Ключові слова: склокристалічні матеріяли, маґнійалюмосилікатні стекла, шпінель, наноструктура, світлопроникність, тріщиностійкість.

(Received 3 December, 2024; in revised form, 9 February, 2025)

1. INTRODUCTION

Nanotechnology is of great importance for both fundamental science and advanced technology [1]. The creation of glass-ceramics based on very small crystallites with volume percent of nanocrystals in it up to more than 90 vol.% was as an example of nanotechnology. Glass-ceramics is a material that consists of a nanocrystalline phase dispersed within the glass matrix. This microstructure can be achieved *via* controlled crystallization of a glass, but the crystal growth rate must be limited [2].

The use of a certain composition of glass and a defined mode of its heat treatment make it possible to synthesize a glass-ceramics with such important properties as chemical, thermal, optical, mechanical and dielectric tailored to particular values [3].

An important class of photonic materials is transparent glass-ceramics, activated by luminescent elements, due to their specific structural, optical and spectroscopic properties [4]. Glass-ceramics, consisting of nanocrystals in a glass phase, become the most promising photonic material for use in tuneable solid-state lasers, luminescent solar concentrators, optical amplifiers and up-conversion luminescence devices, *etc.* [5]. Alternative matrices are spinel crystals of magnesium aluminate ($MgAl_2O_4$) with high thermomechanical properties [6].

Cobalt-doped magnesium–aluminium spinel is an effective material for passive solid-state lasers with a *Q*-switched output operat-

ing in the near-infrared range [7]. To obtain transparent $Co:MgAl_2O_4$ ceramics with a high absorption cross-section and a high linear transmittance, nanopowders of cobalt-doped magnesium-aluminium spinel with a pure phase were synthesized by the co-precipitation method. The 0.05 at.% $Co:MgAl_2O_4$ highly transparent ceramics were obtained after vacuum sintering and hot isostatic pressing (HIP). The HIP post-treated ceramic at 1800°C for 3 h demonstrated the best optical qualities, which were of 81.4% at 400 nm and of 85.9% at 900 nm, as well as the average grain size was of 16.8 μm. Co^{2+} was incorporated into the spinel lattice, as evidenced by broad absorption bands in the wavelength range of 500–700 nm and 1200–1600 nm. However, the limitation of the application of such ceramics is related to the low absorption in the transition range ${}^4A_2(4F) \rightarrow {}_4T_1({}^4F)$ of Co^{2+} ions and, therefore, the low saturated absorption contrast at the generation wavelength [9]. The difficulty of obtaining spinel ceramics is related to the fact that it is very hard to inhibit the growth of the particle size during solid-phase sintering, which significantly affects the change in the optical properties of the materials. In addition, when using pure nanooxide powders for the production of spinel, which allows to reduce the formation temperature and activation energy, the formation of MAS-based materials occurs at high temperatures from 1000°C to 1400°C [10]. Thermoplastic magnesium–aluminate spinel (MAS) nanocomposite developed in Ref. [11] can be shaped *via* polymer injection moulding at high rate and precision. The nanocomposite becomes dense MAS by means of debinding, pre-sintering, and hot isostatic pressing obtaining transparent ceramics with high mechanical strength and high optical transmission up to 84%. However, the limitation of thermoplastic moulding for the production of ceramic materials is the difficulty of obtaining large-size materials and the presence of total porosity (of $\cong 3–5\%$), which can significantly affect the reduction of optical characteristics. In addition, the use of nanooxide powders significantly increases the cost of such materials, and the use of complex technological equipment requires significant changes in the production of ceramic materials. All this inhibits the market entry of nanostructured ceramic materials and limits their competitiveness. Therefore, an important scientific and technical task is the development of new high-tech nanostructured materials based on spinel containing Co^{2+} ions with high absorption in the range of 1.6–1.7 μm.

The prospective use of transparent glass-ceramics is determined by the possibility of providing high light transmission ($T = 72\%$) due to nanostructuring according to the traditional technology of glass production under conditions of low-temperature heat treatment [12]. The high manufacturability and relatively low cost of

glass-ceramics allows it to be effectively used in many fields of science and technology, including photonics, given the fact that their structural or functional elements, namely, clusters, crystallites or molecules, are in the size range from 1 nm to 100 nm [13].

Thus, the authors of Ref. [14] studied thermal, mechanical, and optical properties, in addition to the electron paramagnetic resonance (EPR) spectra and microstructure, for $MgAl_2O_4:Cr^{3+}$ spinel glass and glass-ceramics. The presence of uniform cubic crystals with a size of 10–15 nm in the glass-ceramics was shown by the TEM images. The obtained glass-ceramic samples were characterized by high values of microhardness (6.0 GPa), 3-point flexural strength (of 100 MPa), elastic modulus (of 55 GPa), and fracture toughness (of 5.0 $MPa \cdot m^{1/2}$).

Homogeneous crystallization of crystallites with a size of about 9 nm and not great spherulitic structures consisting of small crystallites ensure the transparency of spinel glass-ceramics with increasing crystallinity. The total amount of nucleating agents ($ZrO_2 + TiO_2$) in the parent glass composition should exceed 5 mol.% for obtaining such a uniform microstructure [15].

For the synthesis of protective transparent high-strength glass-ceramic materials, a methodological approach has been developed that provides transparency in the visible spectral range and high ballistic resistance by fine volumetric crystallization of glass with the formation of a high-strength lithium-disilicate phase of $\cong 50$ vol.% with a size of crystal of ≤ 0.4 μm [12]. The lithium-silicate system was chosen as the initial. The low-temperature two-stage heat treatment was established. It comprises annealing at 723 K for 30 min; stage I—903 K, 30 min; stage II—1123 K, 5 min. The factors that influence on the formation of a fine volumetric crystallized structure under the chosen heat-treatment mode were determined. The ratio of phase-forming oxides is $Li_2O/SiO_2 = 4.0$. There were given the type and quantity of modifying additives SrO, MgO, and CaO, crystallization catalysts ZnO, P_2O_5, and ZrO_2 and fining agents CeO_2 and Sb_2O_3 for the crystallization of glass. The high strength ($HV = 8.74$ GPa, $K_{1C} = 3.1$ $MPa \cdot m^{1/2}$) and light transmission in the visible spectrum ($T = 72\%$) of the developed glass-ceramics were achieved *via* fine volumetric crystallization of glass with the lithium-disilicate content of 45 vol.% and the β-spodumene content of 5 vol.%. However, to create compact lasers on Yb:Er glass, it is necessary to use glass-ceramics, which are characterized by the best parameters of pulses in the passive *Q*-switched mode (PQS). In the model of a laser on Yb:Er glass with lateral diode pumping, this was demonstrated by glass-ceramics based on $Co^{2+}:Mg(Al,Ga)_2O_4$ nanocrystals and based on $Co^{2+}:\gamma\text{-}Ga_2O_3$ nanocrystals [16]. An important drawback is that these glass-ceramic materials differ in

high and long-term temperatures of melting and heat treatment.

Ensuring high performance characteristics (Vickers hardness of 10.4 GPa, fire resistance of 1350°C) and reduced cost due to a two-stage heat treatment at temperatures of 850°C and 1150°C is realized by the determined content and ratio of modifying, glass-forming, and phase-forming components and the introduction into the composition of the combined crystallization catalyst $\Sigma(TiO_2, ZrO_2, CeO_2, P_2O_5)$ with the aim of forming a sitallized structure based on solid solutions of mullite [17]. It has been established that ensuring phase separation at temperatures of 800–850°C by the spinodal mechanism for experimental magnesium–aluminosilicate glass in the pre-crystallization period is an important stage in the formation of solid solutions with the structure of high-temperature quartz in the low-temperature region (850–900°C) with the simultaneous formation of α-quartz and spinel (850–1000°C), which contributes to their recrystallization into α-cordierite (1000–1050°C) and the formation of mullite from α-cordierite at 1100°C [18]. However, although these materials are nanostructured and characterized by a significant spinel content (> 50 vol.%), they are opaque due to the mismatch of the refractive indices of the glass phase and the crystalline phase and the presence of spinel-crystal growth of ≅ 1 μm.

Therefore, in order to develop optically transparent nanostructured spinel-containing glass-ceramic materials, it is important to study the features of their structure formation at the initial stages of nucleation under conditions of low-temperature heat treatment.

2. EXPERIMENTAL PART

2.1. Aim Setting and Research Methodology

The purpose of the work is to study the structure formation of magnesium–aluminosilicate glasses in the process of nucleation and growth of crystals under the conditions of high-speed low-temperature heat treatment.

Investigation of phase transformations in glasses and determination of their heat-treatment temperatures was carried out using gradient-thermal (gradient furnace), petrographic (NU-2e optical microscope with a magnification of 25–1200 times in transmitted light in opaque sections), x-ray phase analysis (DRON-3M diffractometer, Siemens small-angle x-ray diffractometer (radiation source—CuK_α, voltage—30 kV, current—18 mA, set at a point—200 seconds), electron microscopy (Tesla 3 LMU scanning electron microscope with a resolution of 1 nm). The light transmission T [%] of the glass-ceramic material was determined on a FM-94g photometer. The stress intensity coefficient of materials K_{1C} (MPa·m$^{1/2}$) was

determined according to the calculation method [19], which was based on measuring the hardness of samples using PMT-3.

2.2. Rationale for the Selection of Compositions and Synthesis of Glasses for Obtaining Transparent Glass-Ceramic Materials

A glass-ceramics can be transparent in the visible range if it meets one or a combination of the following requirements: the sizes of crystals must be much smaller than the wavelength of visible light (*i.e.*, less than 200 nm); the birefringence must be very low or the difference between the refractive indices of the residual glass matrix and the crystals must be negligible. This applies to most existing transparent glass-ceramics, because they have crystals smaller than 200 nm and a crystallized phase of 1-to-70% [3].

In order to ensure high light transmission ($T \geq 74\%$) and mechanical strength ($HV > 8.0$ GPa, $K_{1C} > 3.0$ MPa·m$^{1/2}$) of transparent glass-ceramic material, it is necessary to provide the following conditions during low-temperature heat treatment:

— the metastable phase separation of glass by the spinodal mechanism in the glass-transition interval;

— the formation of a developed droplet biframe structure near the softening point in a short period of time ($\cong 1$ h);

— the formation of evenly distributed crystalline nuclei in the amount of (10^{12}–10^{15})/cm^3 in the pre-crystallization period;

— the formation of a significant number of crystals > 50 vol.% at the temperature crystallization;

— the inhibition of crystal growth due to high viscosity $\geq 10^8$ Pa·s;

— the formation of a self-organized sitallized nanostructured texture of glass with the size of spinel crystals ≤ 200 nm.

Taking into account the specified criteria to the glass matrix, compositions with PSK marking in the magnesium–aluminosilicate system, which are characterized by a certain content of glass-forming, phase-forming, modifying components and crystallization catalysts (Table 1), were designed with the aim of forming spinel as a crystalline phase that provides high light transmission and mechanical strength.

The choice of phase-forming components in the composition of magnesium–aluminosilicate glasses was based on the classical principles of the sitallized-structure formation of materials and the results of previous developments [18]. In addition, the liquid phase-separation of glass can give an opportunity to control the glass properties and obtain new unique optical materials [20]. Traditionally, to ensure the nucleation and the formation of crystalline phases in the region of lower temperatures, ZnO is introduced into the glass composition, which, along with CeO_2 and P_2O_5, will contribute

TABLE 1. Features of the chemical composition of the PSK series experimental glasses and the crystalline-phase content after heat treatment at temperatures of 850°C and 1000°C for 2 hours.

Marking	Phase-forming and glass-forming components, wt.%				Crystallization catalysts, wt.% P_2O_5, ZnO, ZrO_2, TiO_2, CeO_2, Sb_2O_3	Modifying additives, wt.% SrO, BaO, CaO, CoO	Crystalline phase content
	SiO_2	B_2O_3	MgO	Al_2O_3			
PSK-7	50.0	1.0	10.0	30.0	7.9	2.1	spinel 40 vol.%, α-cristobalite 20 vol.%
PSK-8	45.0	1.0	10.0	35.0	7.9	2.1	spinel 20 vol.%, α-cristobalite 10 vol.%
PSK-9	45.0	1.0	15.0	30.0	7.9	2.1	spinel 20 vol.%, α-quartz 10 vol.%
PSK-10	50.0	4.0	15.0	25.0	4.9	1.1	spinel 40 vol.%, α-quartz 10 vol.%
PSK-11	50.0	4.5	10.0	25.0	7.4	2.1	spinel 20 vol.%, α-quartz 10 vol.%

to the phase separation of glass and the formation of a nanodispersed structure of glass during its heat treatment. The propensity for phase separation of the experimental glasses is determined by the presence of B_2O_3, refractory compounds Al_2O_3 and ZrO_2, and the regulated content of CaO, MgO, SrO, and BaO [18]. As the ionic radius increases in the series MgO > CaO > SrO > BaO, the degree of liquid-phase separation decreases.

It is known that the crystallization temperatures (T_c) of liquid MAS system decreased with the addition of B_2O_3 or P_2O_5 from 764°C to 726°C and 764°C to 750°C, respectively [21]. In order to increase the refractive index of the glass phase, zirconium oxide was introduced as a crystallization catalyst. According to Ref. [22], the vis-

cosity of the glass melt of the MAS system increases with an increase in the concentration of ZrO_2 and CeO_2; so, they were introduced to increase the transparency of the glass.

Experimental glasses with PSK marking in the chosen system were melted in corundum crucibles at temperatures of 1600–1650°C in condition of oxidising atmosphere.

2.3. Study of the Crystallization Nature of Experimental Glasses under Heat Treatment in Relation to Their Light Transmission and Crack Resistance

In order to determine the possibility of spinel crystallization, experimental glasses were treated at the temperatures of nucleation ($T_1 = 850$°C) and crystal growth ($T_2 = 1000$°C) for 2 hours at each stage, which were chosen based on the results of previous studies of the crystallization ability of magnesium–aluminosilicate glasses [12, 17, 18]. After heat treatment, the light-transmission index for PSK-7 glass-ceramics is of 50%; for PSK-8, PSK-9, PSK-11, it is of 70%, and for PSK-10, it is of 72% and is due to the type (Table 1) and the content of the crystalline phase, which was determined using scanning electron microscopy. To obtain optically transparent glass-ceramic materials with high-strength characteristics, which are distinguished by a high crystalline-phase content of ≅80 vol.% and crystal size of ≤0.4 μm, an important condition is the optimization of the heat-treatment mode of the experimental glasses.

The mechanism of nucleation and crystallization of PSK-7 and PSK-10 glasses, which were previously heat-treated at the 'manifestation' temperature (T_{manif}), namely, at 800°C for 1 hour with subsequent holding at temperatures of 850°C, 900°C, 950°C, and 1000°C (Table 2) for 2 hours, were studied to optimize the heat-treatment regime. The 'manifestation' method is based on the crystal growth at the temperature T_{manif}, which originated under heat treatment at lower temperatures. The application of this method is especially valuable for designing the regime of heat treatment of transparent glass-ceramic materials, for which the presence and content of the crystalline phase cannot be determined using traditional methods of gradient–thermal and petrographic methods of analysis and temperatures of crystal formation and growth (Fig. 1).

The influence of the preliminary heat treatment of PSK-7 and PSK-10 glasses at $T_{manif} = 850$°C made it possible to confirm that the pre-crystallization treatment allows to intensify the crystallization and to form a sitallized structure with a crystalline-phase content of 80 vol.%. An important manifestation of the possible phase separation with subsequent nucleation in glasses is the presence of opalescence already at 850°C. This character of phase formation is

TABLE 2. The crystallization ability and the crack resistance of experimental glasses PSK-7 and PSK-10, which were previously 'manifested' at a temperature of 800°C for 1 hour.

Temperature, °C; duration 2 hours	Marking PSK-7	Nature of crystallization*/degree of transparency	K_{1C}, MPa·m$^{1/2}$	Marking PSK-10	Nature of crystallization*/degree of transparency	K_{1C}, MPa·m$^{1/2}$
800		not identified crystalline phase/clear glass	1.5		not identified crystalline phase/clear glass	1.5
850		opalescence	1.5		opalescence	1.5
900		opalescence	2.0		not identified crystalline phase/clear glass	2.4
950		surface crystallization/opaque glass light transmission coefficient 50%	2.0		not identified crystalline phase/clear glass light transmission coefficient 72%	4.8
1000		volume crystallization 80 vol.%/opaque glass	4.0		volume crystallization 80 vol.%/opaque glass	4.3

Notes: *no crystals were detected by x-ray diffraction.

confirmation of the existence of precrystallization liquation and the formation of an optically transparent crystallized structure of PSK-10 glass in the temperature range of 850–900°C. The presence of a crystalline phase in this temperature range is evidenced by the significant content of the crystalline phase at 1000°C. For PSK-7 glass in the temperature range of 850–900°C, there is opalescence, which indicates intensive nucleation and crystal growth already at 950°C.

Confirmation of the transparent sitallized-structure formation is a change in the crack resistance of the experimental materials from 1.5 MPa·m$^{1/2}$ under heat treatment in the temperature range of 800–850°C, when the glasses retain their amorphous structure, to 4.0–4.8 MPa·m$^{1/2}$ under heat treatment in the temperature range of 950–1000°C, when a sitallized structure forms in the glass. Some decrease in the crack-resistance index at a temperature of 1000°C for PSK-10 indicates the crystal growth and destrengthening of the glass structure. In general, the developed glass-ceramic materials are characterized by a higher coefficient of crack resistance compared to spinel-based ceramic materials (≈ 2.0 MPa·m$^{1/2}$) [22], that is possible due to the formation of nanostructured glass.

2.4. Study of Structure Formation

The structure of PSK-7 and PSK-10 glasses at characteristic temperatures was studied to determine the features of phase formation of glasses in relation to performance properties. According to the results of electron microscopy, the PSK-7 glass material at $t_1 = 800°C$ ($\tau = 1$ h) represents a multiphase system formed from a mother glass with spherulites with well-defined boundaries ≅ 100 nm in size (Fig. 1, *a*, I), which combine into agglomerates and ribbons on the general background of nanoinhomogeneities with a size of 10–50 nm (Fig. 1, *b*, II), which may be nuclei of crystallization. The uniformity of the distribution of inhomogeneities in the entire volume of ≅ 50 vol.% is characteristic. The glass material PSK-10,

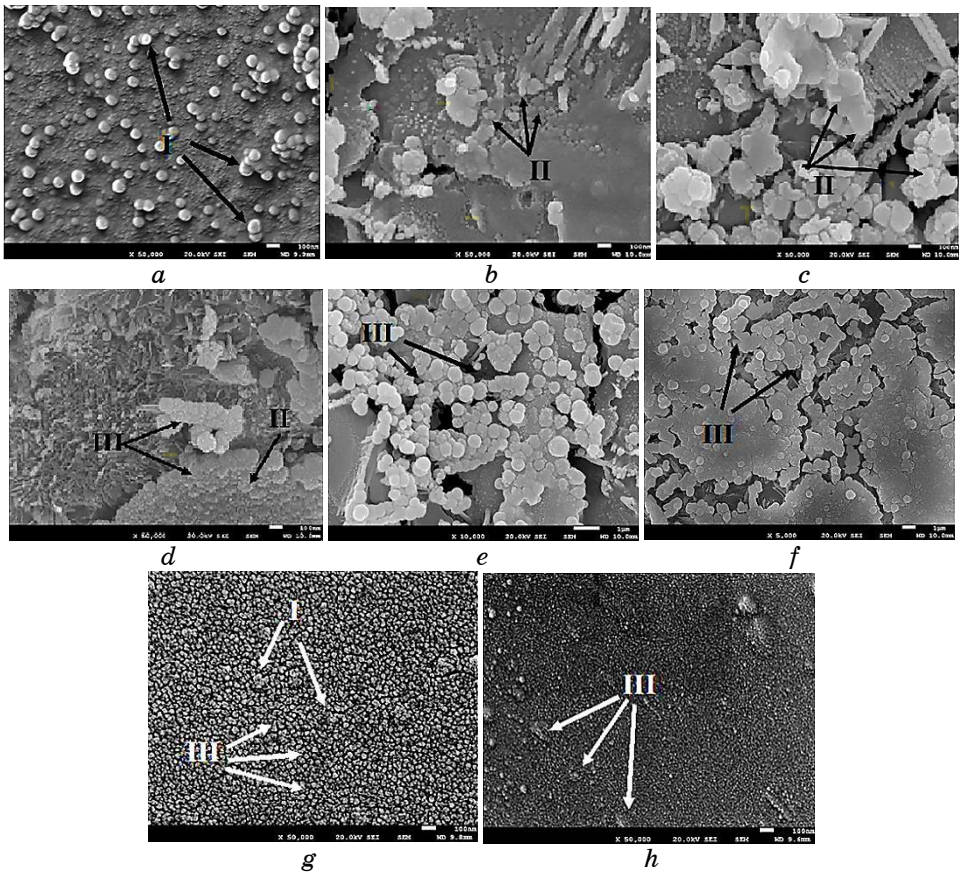

Fig. 1. Structure of experimental glass-ceramic materials after heat treatment: *a*—PSK-7, *b*—PSK-10 at 800°C; *c*—PSK-7, *d*—PSK-10 at 850°C; *e* PSK-7, *f*—PSK-10 at 900°C; *g*—PSK-10, *h*—PSK-7 at 950°C.

which was treated according to the same regime, is characterized by an increase of up to 80 vol.% in the number of spherical inhomogeneities with sizes of 50–100 nm, which are formed based on nanoinhomogeneities with sizes of 10–20 nm. The formation of a significant number of spherulites is an important condition that prevents the further crystal growth with increasing temperature, which can lead to a decrease in light transmission.

When the temperature is increased to $t_2 = 850$°C for the PSK-7 glass material, there is a slight increase in nanoinhomogeneities in the glass structure and their combination in ridges with a size of 100–200 nm (Fig. 1, *c*, II), and the formation of crystallization nuclei on their faces. The difference in the formation of the structure at the initial stages of nucleation for PSK-10 glass material is the increase in the number and the decrease in the size of spherical inhomogeneities with sizes of 50–100 nm (Fig. 1, *d*, II), which form a single interconnected structure. The crystal growth is a characteristic difference of phase separation by the spinodal mechanism, which is manifested in the merging into druses and the coarsening of aggregates (Fig. 1, *d*, III), when the temperature is increased to $t_3 = 900$°C (Fig. 1, *e*, *f*, III). The formation of quartz-like solid solutions and matrix magnesium–aluminosilicate glass are close.

Therefore, in the formed heterogeneous system, sharp boundaries of separation of two phases are not formed that is important for ensuring the light transmission of the material due to the approximation of the refractive indices of the crystalline and glass phases. The dissipative structure of experimental glasses at the stages of nucleation is the main reason for the formation of spinel crystals of an octahedral habit already at $t_4 = 950$°C (Fig. 1, *g*, I). A characteristic feature of PSK-10 glass material is the uniform nature of the distribution of nanocrystals of $\cong 50$ nm size with a content of $\cong 80$ vol.% in the residual glass phase (Fig. 1, *g*, III), which is decisive for ensuring high strength and optical indicators of the glass material. For PSK-7 glass material, some clusters > 200 nm are observed against the background of nanosize crystals (Fig. 1, *h*, III), which can lead to crystal growth and loss of transparency.

The study of the curves of small-angle x-ray scattering (SAXS) phase analysis of PSK-10 and PSK-7 glasses allows us to trace in detail the process of phase separation and nanostructure formation depending on the heat-treatment temperature (Fig. 2).

A significant increase in the intensity $\phi I(\phi)$ of SAXS and, accordingly, the values of the mean square of the difference in the electron densities of the coexisting phases is observed before the appearance of crystalline phases recorded by the x-ray diffraction method (XRD). The formation of a nanoinheterogeneous structure at the initial stages of nucleation is associated with the processes of

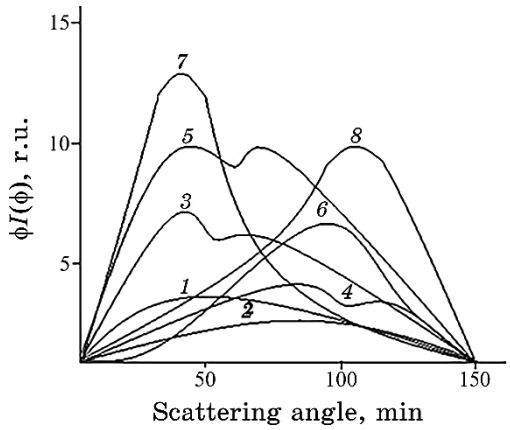

Fig. 2. Dependence of $\phi I(\phi)$ on ϕ (SAXS) during heat treatment of PSK-10 and PSK-7 glasses in the area of metastable liquation and nucleation: *1*, *2*—initial glasses PSK-10 and PSK-7; *3*, *4*—PSK-10 and PSK-7 glasses after heat treatment at a temperature of 800°C; *5*, *6*—PSK-10 and PSK-7 glasses after heat treatment at a temperature of 850°C; *7*, *8*—PSK-10 and PSK-7 glasses after heat treatment at a temperature of 900°C.

metastable liquid-type phase separation. A weakly expressed maximum is observed on the curves of the SAXS of the initial glasses, which indicates the presence of inhomogeneities—sybotaxic groups after the glass melting (Fig. 2, curves *1*, *2*).

In the process of heat treatment, an increase in the intensity of the SAXS and a sharpening of the maximum on the SAXS curves with the highest peak for PSK-10 (Fig. 2, curves *7*, *8*) were observed. This character of SAXS is usually observed with the spinodal mechanism of phase separation, which is associated with the regularity of the distribution of the concentration of the components of the phase that is formed and occurs in the early stages of decomposition. After heat treatment at 800°C, the SAXS curves (Fig. 2, curves *3*, *4*) have two maxima each, which indicate the coexistence of two types of inhomogeneity regions: for PSK-10 glass, a significant number of nanoinhomogeneities is observed near the scattering angle of 50 min, while, for PSK-7, nanoinhomogeneities are concentrated at higher scattering angles near 100 min.

The areas under the curves make it possible to estimate their part in the total volume of the inheterogeneous sample. The observed bidispersity results from metastable separation.

When the processing temperature is increased to 850°C, the tendency to bidispersity is observed after high-temperature heat treatments at the stage of relative stability of the structure (Fig. 2, curve *5*). This means that a relatively stable state of the structure

is achieved at each temperature under the conditions of long-term heat treatment. Thus, in PSK-10 glass, the values and sizes of regions of inhomogeneity grow rapidly up to 850°C and change uniformly at higher temperatures. When the temperature rises to 900°C for PSK-10 glass, the presence of only one phase is recorded, while the structure remains stable (Fig. 2, curve *7*). This may be associated with an increase in the viscosity of the silicate matrix during the separation of phases containing magnesium and aluminium oxides, *i.e.*, with a kinetic inhibition of the phase growth process. Therefore, this structural stability of PSK-10 glass determines the formation of its nanoscale structure during further heat treatment and ensuring high light transmission. For the composition of PSK-7, the SAXS curves have a gentler slope, which indicates an increase in the size of nanoinhomogeneities and the manifestation of monodispersity, when the temperature is increased to 850°C (Fig. 2, curve *6*), that leads to the crystal growth at a temperature of 900°C (Fig. 2, curve *8*) and the decrease in light transmission (Table 2).

Therefore, in the temperature range of 800–850°C, which precedes the crystallization of glass, the metastable liquation immiscibility by the mechanism of spinodal decomposition is observed, which will allow the formation of a finely dispersed structure of glass during heat treatment. Keeping the bidispersity of the system in this interval leads to the structural stability of the glass and the kinetic inhibition of the phase-growth process. The regular nature of the distribution of nanocrystals in the residual glass phase leads to interference effects in scattering x-rays and visible light that allows obtaining a highly transparent glass-ceramic material.

Taking into account the conducted research and previous studies on the development of transparent glass-ceramic materials, the following heat-treatment mode was chosen for obtaining transparent nanostructured spinel-containing glass-ceramic materials: (I stage—$T = 800$°C, $\tau = 60.0$ min; II stage—$T = 900$°C, $\tau = 30$ min; III stage—$T = 950$°C, $\tau = 5$ min).

A transparent nanostructured sitall based on PSK-10 glass with content of 50 vol.% of spinel crystals, which is characterized by light transmission of 72% and a stress-intensity index of 4.8 MPa·m$^{1/2}$, allows it to be considered promising in obtaining of optical materials for laser technology.

4. CONCLUSIONS

The main criteria for ensuring high light transmission and, at the same time, mechanical strength of the magnesium–aluminosilicate glass-ceramic material by forming a self-organized sitallized nanostructured glass texture with a size of spinel crystals of 50 nm

under conditions of low-temperature heat treatment have been determined.

The peculiarities of the formation of optically transparent nanostructured spinel-containing glass-ceramic materials have been established. They consist in: the formation of two types of inhomogeneities with sizes of 10–50 nm and 50–100 nm based on sybotaxic groups by phase separation *via* the spinodal mechanism ($T = 800$°C); stimulation of nucleation during the combination of bidisperse spherulites in the ridge ($T = 850$°C) and the stabilization of the nanostructure by limiting the growth of monodisperse spherulites and their fusion into druses ($T = 900$°C); the formation of a dissipative sitallized structure ($T = 950$°C) due to nanostructuring with the presence of spinel of an octahedral habit with a size of ≅ 50 nm and a content of ≅ 50 vol.% in the residual glass phase, which is decisive for ensuring high strength and optical indicators of the glass material.

The technological parameters for obtaining of a transparent glass-ceramic material based on spinel were selected (stage I—$T = 800$°C, $\tau = 60.0$ min; stage II—$T = 900$°C, $\tau = 30$ min; stage III—$T = 950$°C, $\tau = 5$ min) and a transparent nanostructured sitall with a content of 80 vol.% of spinel crystals, with a light transmission of 72% and a stress-intensity index of 4.8 MPa·m$^{1/2}$ as a basis for functional elements of optics and laser technology was developed.

REFERENCES

1. S. Prakash Singh, M. Li, and H. J. Fecht, *Front. Mater.*, **9**: 869266 (2022); https://doi.org/10.3389/fmats.2022.869266
2. G. A. Khater, E. M. Safwat, J. Kang, Y. Yue, and A. G. A. Khater, *IJRSSET*, **7**, Iss. 3: 1 (2020); http://www.ijrsset.org/pdfs/v7-i3/1.pdf
3. A. Chakrabarti, S. Menon, A. Tarafder, and A. Rahaman Molla, *Glasses and Glass-Ceramics*, **1**: 265 (2022); http://dx.doi.org/10.1007/978-981-19-5821-2_10
4. Yu. C. Teng, K. Sharafudeen, S. Zhou, and J. Qiu, *JCS-Japan*, **120**, No. 1407: 458 (2012); https://doi.org/10.2109/jcersj2.120.458
5. J. M. Pappas, E. C. Kinzel, and X. Dong, *MFGLET*, **24**: 92 (2020); https://doi.org/10.1016/j.mfglet.2020.04.003
6. Y. Qi, Z. Bai, Y. Wang, X. Zhang, Y. Qi, J. Ding, Z. Bai, and Z. Lu, *Infrared Physics & Technology*, **116**: 103727 (2021); https://doi.org/10.1016/j.infrared.2021.103727
7. J. Yanqiu, L. Qiang, S. Sha, L. Xiaoying, L. Ziyu, W. Jingya, and L. Jiang, *Journal of Inorganic Materials*, **36**, Iss. 8: 877 (2021); https://doi.org/10.15541/jim20200679
8. J. Hostaša, *Ceramics for Laser Technologies. Encyclopedia of Materials: Technical Ceramics and Glasses* (Ed. M. Pomeroy) (Elsevier: 2021), vol. **3**, p. 451, p. 110–124; https://doi.org/10.1016/B978-0-12-803581-8.11779-5

9. N. Saheb, S. Lamara, F. Sahnoune, and S. F. Hassan, *SSRG—IJTE*, **20**: 11549 (2022); https://doi.org/10.1007/s10973-022-11344-1
10. Z. Shi, Q. Zhao, B. Guo, T. Ji, and H. Wang, *Mater. Des.*, **193**: 108858 (2020); https://doi.org/10.1016/j.matdes.2020.108858
11. O. Savvova, G. Voronov, V. Topchyi, and Yu. Smyrnova, *Chemistry and Chemical Technology*, **12**, No. 3: 391 (2018); https://doi.org/10.23939/chcht12.03.391
12. G. C. Righini, A. De Pablos-Martín, M. J. Pascual, and M. Ferrari, *La Rivista del Nuovo Cimento*, **201538**, Iss. 7–8: 311 (2015); http://dx.doi.org/10.1393/ncr/i2015-10114-0
13. A. R. Molla, C. R. Kesavulu, R. P. S. Chakradhar, A. Tarafder, S. K. Mohanty, J. L. Rao, B. Karmakar, and S. K. Biswas, *Journal of Alloys and Compounds*, **583**: 498 (2014); https://doi.org/10.1016/j.jallcom.2013.08.122
14. A. L. Mitchell and C. M. Smith, *Journal of the American Ceramic Society*, **103**, Iss. 9: 4925 (2020); https://doi.org/10.1111/jace.17129
15. Y. Shi, C. Gao, Q. Ye, S. Wang, Q. Wang, M. Gao, P. Loiko, N. Skoptsov, O. Dymshits, A. Zhilin, S. Zapalova, M. Tsenter, V. Vitkin, X. Mateos, and K. Yumashev, *Laser Physics Letters*, **15**: 4 (2018); http://dx.doi.org/10.1088/1612-202X/aaa9a8
16. V. O. Savvova, S. M. Logvinkov, O. V. Babich, and A. R. Zdorik, *Voprosy Khimii i Khimicheskoi Tekhnologii*, **3**: 96 (2018).
17. O. V. Savvova, H. K. Voronov, O. I. Fesenko, V. D. Tymofieiev, and O. I. Pylypenko, *Nanosistemi, Nanomateriali, Nanotehnologii*, **20**, Iss. 3: 667 (2022); https://doi.org/10.15407/nnn.20.03.667
18. O. V. Savvova, O. V. Babich, G. K. Voronov, and S. O. Ryabinin, *Visokomitsni Spodumenovi Sklokristalichni Materiali* [High-Grade Spodumene Glass-Crystalline Materials] (Kyiv: G. S. Pisarenko Institute for Problems of Strength, N.A.S. of Ukraine: 2017) (in Ukrainian).
19. Alexander Veber, Zhuorui Lu, Manuel Vermillac, Franck Pigeonneau, Wilfried Blanc, and Laeticia Petit, *Fibers*, **7**, Iss. 12: 105 (2019); https://doi.org/10.3390/fib7120105
20. Z. Hong Bao, L. Feng Miao, W. Hui Jiang, and J. Min Liu, *Materials Science Forum*, **848**: 243 (2016); https://doi.org/10.4028/www.scientific.net/MSF.848.243
21. M. D. Karkhanavala and F. A. Hummel, *Journal of the American Ceramic Society*, **36**, Iss. 12: 389 (2006); https://doi.org/10.1111/j.1151-2916.1953.tb12825.x
22. S. Honda, Y. Ogihara, A. Ikesue, Y. Lin Aung, S. Hashomoto, and Y. Iwamoto, *Journal of Asian Ceramic Societies*, **11**, Iss. 4: 451 (2023); https://doi.org/10.1080/21870764.2023.2248714